Assessment of Optic Pathway Structure and Function in Patients With Compression of the Optic Chiasm: A Correlation With Optical Coherence Tomography

Pramit M. Phal,[1,2] Christopher Steward,[2,3] Andrew D. Nichols,[4] Chris Kokkinos,[1] Patricia M. Desmond,[2,3] Helen Danesh-Meyer,[5] Yuval Z. Sufaro,[6,7] Andrew H. Kaye,[6,7] and Bradford A. Moffat[8]

[1]Epworth Medical Imaging, Epworth Hospital, Richmond, Victoria, Australia
[2]Department of Radiology, The University of Melbourne, Parkville, Victoria, Australia
[3]Department of Radiology, Royal Melbourne Hospital, Parkville, Victoria, Australia
[4]Department of Neurosurgery, Alfred Health, Prahran, Victoria, Australia
[5]Department of Ophthalmology, The University of Auckland, Auckland, New Zealand
[6]Department of Neurosurgery, The University of Melbourne, Parkville, Victoria, Australia
[7]Department of Neurosurgery, Royal Melbourne Hospital, Parkville, Victoria, Australia
[8]Department of Anatomy and Neuroscience, Melbourne Neuroscience Institute, The University of Melbourne, Parkville, Victoria, Australia

Correspondence: Bradford A. Moffat, Department of Anatomay and Neuroscience, MDHS, Kennth Myer Building, 30 Royal Parade, The University of Melbourne, Parkville, VIC 3010, Australia; bmoffat@unimelb.edu.au.

Submitted: November 25, 2015
Accepted: March 10, 2016

Citation: Phal PM, Steward C, Nichols AD, et al. Assessment of optic pathway structure and function in patients with compression of the optic chiasm: a correlation with optical coherence tomography. *Invest Ophthalmol Vis Sci*. 2016;57:3884–3890. DOI:10.1167/iovs.15-18734

Purpose. The purpose of this study was to investigate correlations between retinal fiber thickness measured by optical coherence tomography (OCT) and anterograde functional and structural differences in the optic pathway of patients with compression of the optic chiasm. Our hypothesis was that loss of visual acuity caused by chronic compressive pathologies may lead to an irreversible decline in vision because of permanent neurodegeneration of the optic radiations and visual cortex.

Methods. Quantitative OCT, functional magnetic resonance imaging (MRI) and diffusion tensor MRI measurements were made in 17 patients being surgically treated for chiasmal compression.

Results. In our study we found that surgically irreversible visual field defects and reduced retinal nerve fiber layer thickness were significantly associated with lower fractional diffusion anisotropy and higher diffusivities in optic radiations and less functional MRI activation in the visual cortex.

Conclusions. Damage to the retinal nerve fiber layer is associated with downstream structural and functional degradation of the optic pathway. This may be related to trans-synaptic degeneration and the fact that these factors are important potential imaging biomarkers for predicting visual recovery after surgical decompression.

Keywords: compressive optic neuropathy, diffusion MRI, optical coherence tomography,

Pituitary tumors are relatively common, accounting for 10% to 15% of primary brain tumors.[1] When these tumors are large, they grow into the suprasellar cistern and can lead to compression of the optic chiasm, with consequent visual defects,[2,3] as can happen with other tumors in this region, such as meningioma and craniopharyngioma. As such, an important aspect of their clinical management is surgical decompression of the optic chiasm. However, a significant number (~20%) of patients do not gain an appreciable improvement in their visual acuity.[4] Given this scenario, it is desirable to prospectively predict which patients will respond to surgery. A variety of prognostic factors have been described. Optical coherence tomography (OCT) demonstrates a correlation between reduced retinal nerve fiber layer (RNFL) thickness and visual field defects on perimetry in patients with compression of the optic chiasm[5] and is predictive of visual recovery after surgical decompression of the optic chiasm.[6,7] Currently, however, there is a paucity of knowledge regarding the "downstream" effects of compression of the optic chiasm, that is, effects on the optic radiations (OR) and on primary visual cortex (V1).

Diffusion-weighted magnetic resonance imaging (MRI) allows for the noninvasive quantification of the restricted random motion (Brownian motion) of water molecules[8] in the human brain. This mode has clinical utility in acute stroke imaging and imaging other neurological disease including intracranial infection, demyelination, and brain tumors because a loss of cellular homeostasis results in measurable changes to this restricted motion. In the coherently aligned myelinated white matter fibers, diffusion is least restricted parallel to the fibers and maximally restricted perpendicular to the fibers. This is called anisotropic diffusion[9] and is modeled mathematically by 3×3 matrix or tensor. As such, diffusion MRI is able to image cellular structures such as cell membranes and myelin, which exhibit directional impedance to water diffusion. Diffusion tensor imaging is used clinically in tractography, particularly in planning surgery, and has demonstrated good success in depicting optic radiations, including the anterior-

Investigative Ophthalmology & Visual Science

most curved aspect, "Meyer's loop."[10,11] From the diffusion tensor dataset, parameters such as fractional anisotropy and mean diffusivity allow assessment of integrity of white matter pathways and allow for quantitative analysis. Diffusion tensor imaging (DTI) is therefore ideally suited for use as a quantitative biomarker in assessing optic radiations.

Functional MRI (fMRI) with blood oxygenation level-dependent (BOLD) imaging is an indirect measure of neuronal activity. Its physical basis relies upon the differing magnetic properties of oxyhemoglobin, which is diamagnetic, and deoxyhemoglobin, which is paramagnetic. Increased neuronal activity leads to increased blood flow to the active region, as predicted by the hemodynamic response function,[12] resulting in differing concentrations of oxy- and deoxyhemoglobin in active regions compared to those in nonactive regions. Functional MRI performed with a paradigm for visual activation demonstrates robust activation of the lateral geniculate nuclei (LGN) and visual cortex.[13] Studies performed at higher magnetic field strength and with higher resolution demonstrate a columnar organization of the primary visual cortex.[14] Although fMRI is ideally suited to assessment of visual pathways, there has been little published to date on the effects of chiasmal compression on activation within the visual cortex.

With these factors in mind, the aim of this study was to use advanced diffusion tensor MRI and fMRI to investigate the structural and functional differences in the OR and visual cortex between postsurgical pituitary tumor patients with and without persistent visual field deficits. Our hypothesis was that visual loss preceding surgical intervention may cause synaptic degradation through lack of use, resulting in irreversible visual loss. In addition, if this degradation was significant enough, it should be detectable using advanced MRI acquisition and quantification strategies, namely diffusion tensor parameters within the OR and BOLD response to visual fMRI paradigms in the visual cortex.

Methods

Melbourne Health Human Research Ethics Committee approval was obtained for this study, which is a substudy of the of Longitudinal Evaluation of Retinal Nerve Fiber Layer and Visual Field Sensitivity as Measured by Optical Coherence Tomography and Magnetic Resonance Imaging in Chiasmal Compression, being conducted at the Royal Melbourne and Royal Melbourne Private Hospitals. Seventeen patients who had undergone surgery at least 12 months previously for tumors causing compression of the optic chiasm were recruited and reviewed by an ophthalmologist. Fifteen of these subjects had pituitary macroadenomas resected using a trans-sphenoidal approach, and singular cases of craniopharyngioma and suprasellar meningioma resected via craniotomy. A comprehensive table of clinical, pathology, and radiological information is provided in Supplementary Table S1. The study population consisted of 10 patients with no visual deficits (ND; visual field deviation > -5 dB from age-matched controls and a normal average RNFL thickness >75 microns) and 7 patients with significant visual deficits (VD) (confirmed bitemporal hemianopia, visual field deficit < -5dB from age-matched controls and average RNFL thinning <75 μm, measured by using OCT [Stratus model; Zeiss, Jena, Germany). Patients with contraindications to MRI (implantable devices and claustrophobia) and noninterpretable MRI studies were excluded.

All patients underwent additional MRI scans performed using a Trio 3T MRI unit (Siemens, Erlangen, Germany) with a 12-channel head coil. Anatomic imaging included nonvolumetric FLAIR imaging and volumetric MPRAGE sequences (field of view [FOV] = 200 × 160 mm; matrix = 512 × 256; voxel size = 0.39 × 0.78 × 1.5 mm; TE = 5.1 ms; TR = 16.2 ms; 124 slices with slice gap of 0 mm). Diffusion tensor MRI consisted of 64 direction (b = 0.3000), 55 slices with 2.5- × 2.5- × 2.5-mm isotropic voxels (TR/TE = 8000/80 ms); 10-minute acquisition time. Functional MRI (FOV = 200 × 200; matrix = 64 × 64; voxel = 3 × 3 × 3 mm; TE = 25.3 ms; TR = 2500 ms; 36 slices with slice gap of 0 mm) were acquired using clinical fMRI equipment (MRIχ Technologies, Bannockburn, IL, USA)[15] and software to present a visually guided saccade for 30 seconds interleaved with 30 seconds of rest (repeated four times).[16]

Diffusion and fMRI data sets then underwent spatial normalization to the MNI152 standard brain,[17] using a 12-parameter affine coregistration algorithm (MINC tools; McConnell Brain Imaging Centre, http://www.bic.mni.mcgill.ca/ServicesSoftware/MINC, available in the public domain),[18] and all datasets underwent rigorous quality assurance by an MR physicist (B.A.M.). A previously established and validated automatic diffusion tractography algorithm[10] was then used to identify and segment the OR. An LGN seed, a V1 target, ipsilateral exclusion zone, and mid-OR way points in MNI space were resampled in native diffusion space, using the results of the spatial normalization. Constrained spherical deconvolution and probabilistic tractography was then used to calculate the trajectories of fibers within the OR (see Fig. 2a). OR tract images (see Fig. 2b) were then calculated by thresholding the relative track density images at 5%.

In the resultant tractography images, a region of interest (ROI) in the coronal plane was created at the midpoint between the anterior point of Meyer's loop and the occipital pole of the ipsilateral hemisphere. Mean radial diffusivity (RD), axial diffusivity (AD), mean diffusivity (MD), and fractional anisotropy (FA) in this ROI were then calculated. The region was chosen because it was an area with minimal crossing and bending white matter fibers that can confound and/or reduce the specificity of FA as a biomarker of white matter structural integrity. All diffusivity values are units of $\times 10^9$ m^2/s.

To quantitatively process fMRI data, we identified both the left and the right V1 cortices according to the Talairach atlas (Talairach.org; http://www.talairach.org/daemon.html, available in the public domain), and probability images (thresholded at 10%) were resampled in fMRI space. The time course MRI signal in this ROI was then normalized by converting z scores based on the temporal mean and standard deviations. For each subject and V1 ROI, a t score was calculated by using a pairwise comparison of the z scores during visually guided saccade activation and those during the rest periods, using Matlab software (Mathworks, Danvers, MA, USA) statistical toolbox.

Statistical comparisons of MRI results between patients with and without RNFL thinning were performed using Prism (GraphPad Software, Inc., La Jolla, CA, USA). Because data were not normally distributed and the numbers of subjects in each group were modest, the Mann-Whitney U test for independent samples was used to test for significant group differences. In addition, a stepwise nonparametric regression analysis was performed to investigate the relationships among preoperative VF and RNFL measurements and FA. Values of VF, RNFL, and FA were ranked, and the ranked values were entered into a stepwise regression algorithm (Matlab; Mathworks).

Results

Seventeen patients with compressive pathology were recruited to undergo prospective RNFL and advanced MRI investigations of their optic pathways. Figure 1 shows an example of the

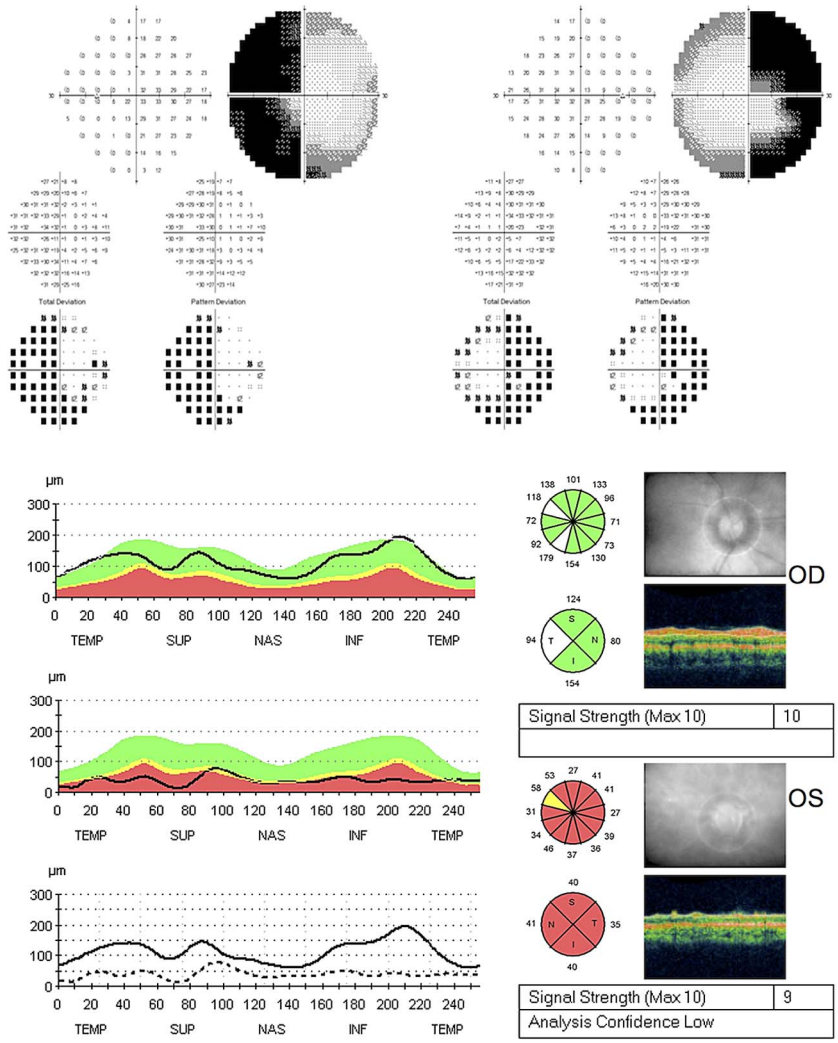

Figure 1. Humphrey visual field testing demonstrated bitemporal hemianopia, and OCT showed reduced RNFL thickness on the left.

optical results reported for each patient. In this subject, it can be seen that the bilateral temporal visual field deficits are associated with thinning of the left RNFLs. This is consistent with more exhaustive studies showing a correlation.[5–7]

Results of the diffusion tensor MRI acquisition and analyses can be seen in Figure 2. For quality assurance purposes, whole-brain tractography was performed in addition to OR tractography. In the images of the raw tractography example (Fig. 2a), it can be seen that most reconstructed tracks follow the optic pathway; however, there always remained some false positive tracks. To remove them, maps of the track density (images where the intensity is represented by the number of tracks passing through each pixel) were calculated and then thresholded at 5% of the maximum density (Fig. 2b). The coronal plane at the midpoint of the OR (Fig. 2b) consistently contained voxels with minimal crossing tracks from non-OR tracts. Therefore this was the ROI used to generate the summary diffusion tensor results for each subject.

The median AD (10.2) of the VD group was found to be significantly ($P = 0.03$) greater than that of the ND group (9.6), with a U value of 78 (Fig. 2c). The median MD (9.0) of the VD group was found to be significantly ($P = 0.04$) greater than that of the ND group (8.7) and had a U value of 82 (Fig. 2c). The median FA (0.38) of the VD group was found to be significantly ($P = 0.03$) less than that of the ND group (0.39), with a U value of 47 (Fig. 2c). The median RD (6.4) of the VD group was found to be significantly ($P = 0.01$) greater than that of the ND group (6.0), with a U value of 69 (Fig. 2c). In addition, a stepwise multiple regression found the preoperative RNFL values were significantly ($P < 0.0001$) correlated (rho = 0.58) with FA. Preoperative VF was also correlated to FA but was not found to be significantly ($P = 0.7$) independent of RNFL. Plots of RNFL and VF rank as a function of FA can be seen in the Supplementary Figures S1 and S2.

To quantify the activation of V1 (Fig. 3a) during a visual stimulus, the normalized increase in BOLD fMRI signal was calculated and converted to mean t-scores. These t-scores (Fig. 3b) were then statistically compared between the VD and ND groups. It was found that the median t-score activation of the VD group (2.6) was significantly ($P = 0.02$) less than that of the ND group (5.1) with a U value of 53.

Discussion

This study investigated, for the first time, anterograde transsynaptic differences in the OR associated with optic chiasm compression by using advanced diffusion tensor MRI and fMRI. Associated with reduced RNFL was evidence of reduced fiber integrity in the optic radiations, as assessed by lower fractional anisotropy and higher diffusion tensor values of the parameters

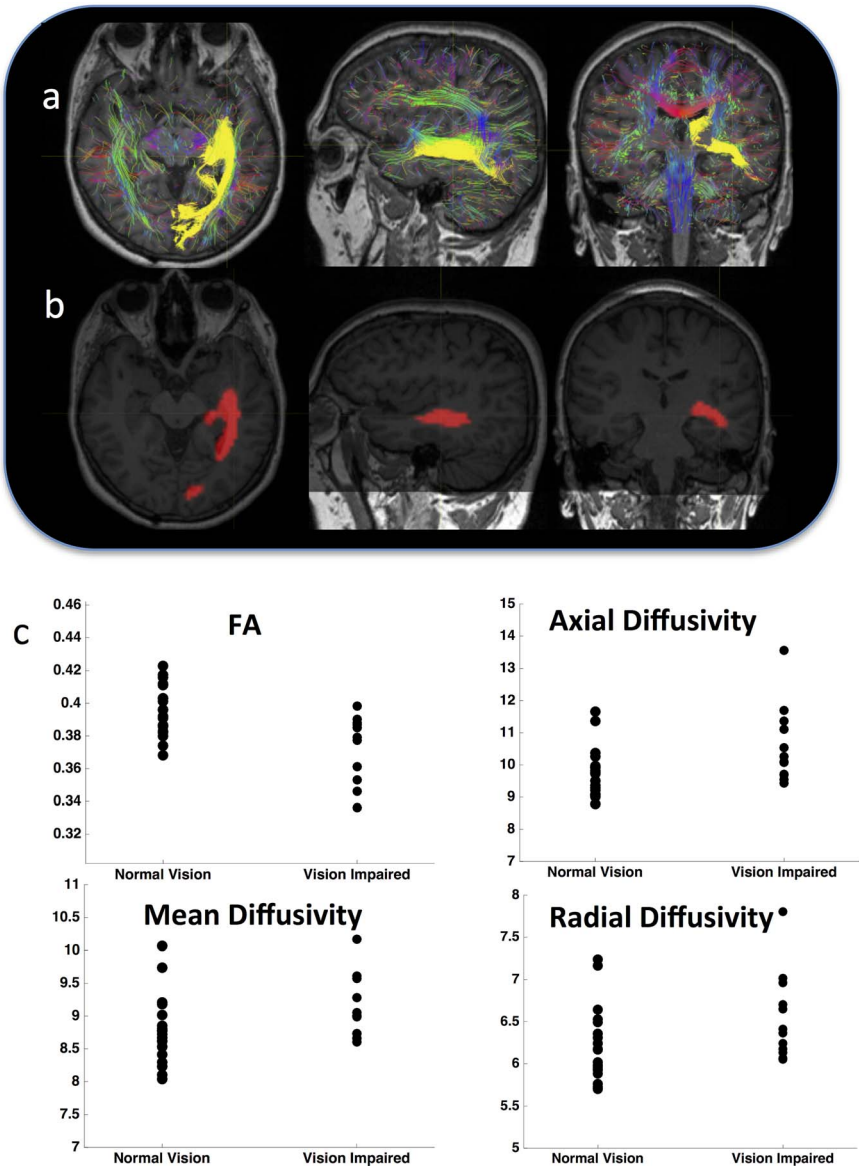

FIGURE 2. Diffusion MRI results. (**a**) White matter tractography of the whole brain and of the optic radiations (*yellow*) overlaid onto anatomical MR images. (**b**) Track density images of the optic radiations thresholded at 5%. (**c**) Jitter plots of FA, AD, RD, and MD comparing normal and abnormal vision groups postoperatively.

AD, RD, and MD, and lower visual cortical activation as measured by BOLD signal during a visual activation fMRI paradigm.

Visual pathways can be divided into anterior segment, consisting of retinal ganglion cells, optic nerve, optic chiasm, and optic tracts and posterior segment, consisting of the optic radiations and visual cortex. These divisions connect through the lateral geniculate nucleus within the posterior thalamus, where the axons synapse. The phenomenon of a process in one part of the visual pathway affecting the other is known as trans-synaptic degeneration because it requires transmission through the synapse within the lateral geniculate nucleus.[19] The time course for this in humans has recently been elucidated,[20] and there is evidence of this degeneration occurring in both a retrograde and an anterograde manner. For example, processes involving the retina such as glaucoma have been shown to result in reduced cortical thickness in the visual cortex, occurring through a range of clinical severity but most marked in the end stages of disease.[21–23] Patients with pathology in the posterior visual pathway, such as those with infarction in the territory of the posterior cerebral artery, demonstrate reduced RNFL thickness.[24] Furthermore, patients with multiple sclerosis and lesions in the optic radiations demonstrate both reduced RNFL thickness and visual cortical atrophy.[19] In our patient group with chiasmal compression and no visual recovery following surgery, it is likely that there was trans-synaptic degeneration occurring. The retrograde effect of chiasmal compression was already well recognized with reduced RNFL thickness[5]; in our study, we have delineated the downstream effects on both the optic radiations and the visual cortex.

With respect to the disordered diffusion tensor parameters (FA, AD, RD, MD) in the postsurgical visual deficit group in our study, an important consideration is to correlate what these different diffusion tensor parameters are believed to represent on a cellular level. Fractional anisotropy, expressed as a numerical value between 0 and 1, is a measure of the directionality of diffusion in the imaged voxel.[25] Axial and

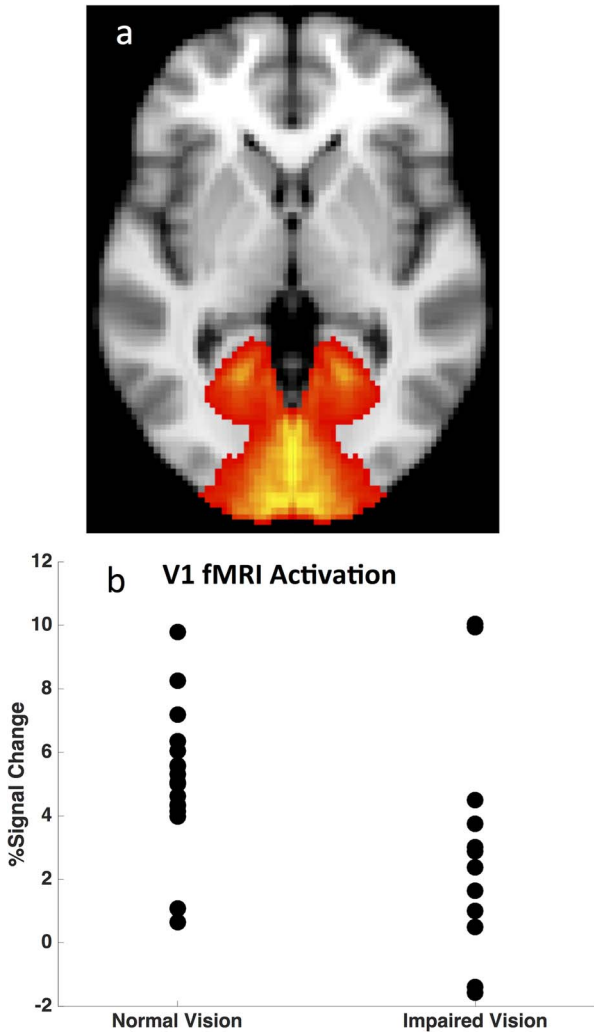

FIGURE 3. (**a**) Region of interest shows area V1 overlaid on the MNI152 standard brain. This region was used to quantify fMRI activation during a visual stimulus presentation paradigm. (**b**) Jitter plot comparing area V1 activation in normal group with that in abnormal group.

radial diffusivity describe diffusion in relation to the principal eigenvector; in our study, this reflects diffusion along and perpendicular to the neuron. In a rat model of ischemia of the optic nerve, it has been postulated that axial diffusivity reflects axonal integrity (related to ischemia), whereas radial diffusivity is a representation of myelination.[26] It is therefore feasible that the abnormal vision group in our study had both ischemic and demyelinating changes occurring in neurons within the optic radiations.

Our study is the first to assess the effects of chiasmal compression on the posterior visual pathways. This novel finding supports an anterograde trans-synaptic degeneration of the visual pathway distal to anatomically distorted optic chiasm by suprasellar lesions. This compliments a prior study using DTI to investigate the optic tracts anterior to the LGN synaptic junction in patients with chiasmal compression.[27] The study found that patients with chiasmal compression had reduced FA and increased AD and RD values in the optic tracts, and this correlated with the degree of postsurgical visual recovery, postulating that recovery corresponded to postsurgical "re-myelination" of the optic tracts. Interestingly, the study by Paul et al.[27] found that changes in RD and FA but not AD correlated with VF recovery. The decrease in RD at 4 weeks postsurgery was suggestive of rapid remyelination of the optic tract. Our study findings imply that there may be more permanent and severe trans-synaptic degeneration of the OR occurring in patients with the most severe presurgical visual deficits, as shown by both lower AD and RD.

There was another prior study that used diffusion tensor MRI to assess the optic radiations of glaucoma patients.[28] That study showed reduced FA in the optic radiations that correlated with the clinical severity of glaucoma.[28] Diffusion tensor imaging has also found utility in assessing degenerative processes outside the visual pathways. For example, in the assessment of the early stages of Wallerian degeneration of the motor tracts post ischemic stroke, it has been demonstrated that a decrease in FA is evident earlier than the increased T2 signal and atrophy within the cerebral peduncle.[29] To date there have been no studies of the utility of serial DTI as a putative biomarker in the posterior visual pathways.

Our study demonstrated decreased activation in the visual cortex in the group of patients who did not recover vision after chiasmal decompressive surgery. This finding may be the end result of decreased retinal ganglion cells or caused by decreased integrity of the optic radiations, or a combination of both of these factors. Other studies have demonstrated decreased visual cortical activation due to anterior pathway lesions, including that due to lens abnormalities[30] and glaucoma,[31] as well as in binocular rivalry.[32] Decreased visual cortical activation in lens-induced myopia is of considerable practical importance in clinical task-based MRI studies and highlights the need to correct this before the study being performed.[30]

Many factors have been investigated in predicting visual recovery after optic chiasm decompression surgery. Reduced RNFL thickness, which reflects irreversible damage to retinal ganglion cells, has been demonstrated to be a reliable predictor of poor visual recovery after surgery.[6] Other factors, including length of symptoms, age, tumor size, preoperative visual fields, and visual acuity demonstrate conflicting evidence,[33–37] morphological recovery of the optic chiasm[38] and the nature of chiasmal distortion.[39] Assessment of optic atrophy, although somewhat predictive of recovery,[35] is notoriously subjective.[6,37] Findings in our study show evidence of Wallerian degeneration in the optic radiations and lower visual cortical activation on fMRI, as found also in the study by Paul et al.,[27] showing evidence of optic tract remyelination, which provides good impetus to study these findings as potential biomarkers in predicting recovery after chiasmal decompressive surgery—and this will be the subject of a proposed follow-up study. It is our opinion that investigation of the optic radiation has several advantages: it is a large white matter structure that can be automatically segmented using diffusion-weighted imaging data[10]; diffusion-weighted imaging data within it do not suffer distortion and misregistration from anatomical images, unlike the optic tract region, which is adjacent to bone; and therefore has the potential to be more robust and clinically translatable.

The primary limitation of our study is the small number of patients, which leads to the possibility that subtle differences between the groups may not be detected. Recruiting more numbers would mean that additional analyses could be performed, such as comparing cortical thickness between groups, a task that requires larger numbers to detect changes between the groups.[40] In addition, our study involved a single postoperative time point. A more comprehensive study using DTI and fMRI both pre- and postoperatively could further establish these parameters as biomarkers in predicting postoperative visual recovery.

Conclusions

In our study we found that optic chiasmal compression with visual field defects and reduced RNFL thickness was associated with lower FA in optic radiations and lower activation of the visual cortex. We believe that this condition is related to transsynaptic degeneration, which may have a mechanism different from those of reversible presynaptic degeneration of the optic tract[27] and RNFL.[5–7] The mechanism of such neurodegeneration is unknown, however, studies in animal models have found evidence of apoptosis in the LGN and visual cortex following optic nerve injury.[41]

These factors may be important in understanding postsurgical decompression. A larger and more comprehensive study is required to determine which of and how all these biomarkers should be combined to appropriately manage patients with optic chiasmal compression.

Acknowledgments

Supported by the Royal Melbourne Hospital Neuroscience Foundation, Australian National Health and Medical Research Council Grants 454790 and 566992, and the University of Melbourne node of the Australian National Imaging Facility.

Disclosure: **P.M. Phal**, None; **C. Steward**, None; **A.D. Nichols**, None; **C. Kokkinos**, None; **P.M. Desmond**, None; **H. Danesh-Meyer**, None; **Y.Z. Sufaro**, None; **A.H. Kaye**, None; **B.A. Moffat**, None

References

1. Müller-Forell W. Intracranial pathology of the visual pathway. *Eur J Radiol*. 2004;49:143–178.
2. Cushing H, Walker CB. Distortions of the visual fields in cases of brain tumour: chiasmal lesions, with especial reference to bitemporal hemianopsia. *Brain*. 1915;37:341–400.
3. Ogra S, Nichols AD, Stylli S, Kaye AH, Savino PJ, Danesh-Meyer HV. Visual acuity and pattern of visual field loss at presentation in pituitary adenoma. *J Clin Neurosci*. 2014;21:735–740.
4. Laws E, Trautmann J, Hollenhorst R. Transsphenoidal decompression of optic-nerve and chiasm—visual results in 62 patients. *J Neurosurg*. 1977;46:717–722.
5. Danesh-Meyer HV, Carroll SC, Foroozan R, et al. Relationship between retinal nerve fiber layer and visual field sensitivity as measured by optical coherence tomography in chiasmal compression. *Invest Ophthalmol Vis Sci*. 2006;47:4827–4835.
6. Danesh-Meyer HV, Papchenko T, Savino PJ, Law A, Evans J, Gamble GD. In vivo retinal nerve fiber layer thickness measured by optical coherence tomography predicts visual recovery after surgery for parachiasmal tumors. *Invest Ophthalmol Vis Sci*. 2008;49:1879–1885.
7. Danesh-Meyer HV, Wong A, Papchenko T, et al. Optical coherence tomography predicts visual outcome for pituitary tumors. *J Clin Neurosci*. 2015;22:1098–1104.
8. Dong Q, Welsh RC, Chenevert TL, et al. Clinical applications of diffusion tensor imaging. *J Magn Reson Imaging*. 2004;19:6–18.
9. Mukherjee P, Berman JI, Chung SW, Hess CP, Henry RG. Diffusion tensor MR imaging and fiber tractography: theoretic underpinnings. *AJNR Am J Neuroradiol*. 2008;29:632–641.
10. Lim JC, Phal PM, Desmond PM, et al. Probabilistic MRI tractography of the optic radiation using constrained spherical deconvolution: a feasibility study. *PLoS One*. 2015;10:e0118948.
11. Mandelstam SA. Challenges of the anatomy and diffusion tensor tractography of the Meyer loop. *AJNR Am J Neuroradiol*. 2012;33:1204–1210.
12. Logothetis NK, Pauls J, Augath M, Trinath T, Oeltermann A. Neurophysiological investigation of the basis of the fMRI signal. *Nature*. 2001;412:150–157.
13. van Heerden J, Desmond PM, Phal PM. Functional MRI in clinical practice: a pictorial essay. *J Med Imaging Radiat Oncol*. 2014;58:320–326.
14. Nemani AK, Atkinson IC, Thulborn KR. Investigating the consistency of brain activation using individual trial analysis of high-resolution fMRI in the human primary visual cortex. *Neuroimage*. 2009;47:1417–1424.
15. Thulborn KR, Davis D, Erb P, Strojwas M, Sweeney JA. Clinical fMRI: implementation and experience. *Neuroimage*. 1996;4(3 Pt 3):S101–S107.
16. Ming J, Thulborn KR, Szlyk JP. Reproducibility of activation maps for longitudinal studies of visual function by functional magnetic resonance imaging. *Invest Ophthalmol Vis Sci*. 2012;53:6153–6163.
17. Mazziotta JC, Toga AW, Evans A, Fox P, Lancaster J. A probabilistic atlas of the human brain: theory and rationale for its development. The International Consortium for Brain Mapping (ICBM). *Neuroimage*. 1995;2:89–101.
18. Collins DL, Neelin P, Peters TM, Evans AC. Automatic 3D intersubject registration of MR volumetric data in standardized Talairach space. *J Comput Assist Tomogr*. 1994;18:192–205.
19. Gabilondo I, Martinez-Lapiscina EH, Martinez-Heras E, et al. Trans-synaptic axonal degeneration in the visual pathway in multiple sclerosis. *Ann Neurol*. 2014;75:98–107.
20. Jindahra P, Petrie A, Plant GT. The time course of retrograde trans-synaptic degeneration following occipital lobe damage in humans. *Brain*. 2012;135(Pt 2):534–541.
21. Bogorodzki P, Piatkowska-Janko E, Szaflik J, Szaflik JP, Gacek M, Grieb P. Mapping cortical thickness of the patients with unilateral end-stage open angle glaucoma on planar cerebral cortex maps. *PLoS One*. 2014;9:e93682.
22. Yu L, Xie B, Yin X, et al. Reduced cortical thickness in primary open-angle glaucoma and its relationship to the retinal nerve fiber layer thickness. *PLoS One*. 2013;8:e73208.
23. Yu L, Xie L, Dai C, et al. Progressive thinning of visual cortex in primary open-angle glaucoma of varying severity. *PLoS One*. 2015;10:e0121960.
24. Park HY, Park YG, Cho AH, Park CK. Transneuronal retrograde degeneration of the retinal ganglion cells in patients with cerebral infarction. *Ophthalmology*. 2013;120:1292–1299.
25. Chung HW, Chou MC, Chen CY. Principles and limitations of computational algorithms in clinical diffusion tensor MR tractography. *AJNR Am J Neuroradiol*. 2011;32:3–13.
26. Song SK, Sun SW, Ju WK, Lin SJ, Cross AH, Neufeld AH. Diffusion tensor imaging detects and differentiates axon and myelin degeneration in mouse optic nerve after retinal ischemia. *Neuroimage*. 2003;20:1714–1722.
27. Paul DA, Gaffin-Cahn E, Hintz EB, et al. White matter changes linked to visual recovery after nerve decompression. *Sci Transl Med*. 2014;6(266):266ra173.
28. Chen Z, Lin F, Wang J, et al. Diffusion tensor magnetic resonance imaging reveals visual pathway damage that correlates with clinical severity in glaucoma. *Clin Exp Ophthalmol*. 2013;41:43–49.
29. Thomalla G, Glauche V, Koch MA, Beaulieu C, Weiller C, Rother J. Diffusion tensor imaging detects early Wallerian degeneration of the pyramidal tract after ischemic stroke. *Neuroimage*. 2004;22:1767–1774.
30. Mirzajani A, Sarlaki E, Kharazi HH, Tavan M. Effect of lens-induced myopia on visual cortex activity: a functional MR imaging study. *AJNR Am J Neuroradiol*. 2011;32:1426–1429.
31. Qing G, Zhang S, Wang B, Wang N. Functional MRI signal changes in primary visual cortex corresponding to the central

normal visual field of patients with primary open-angle glaucoma. *Invest Ophthalmol Vis Sci*. 2010;51:4627–4634.

32. Lee SH, Blake R. V1 activity is reduced during binocular rivalry. *J Vis*. 2002;2:618–626.
33. Powell M. Recovery of vision following transsphenoidal surgery for pituitary adenomas. *Br J Neurosurg*. 1995;9:367–373.
34. Findlay G, McFadzean RM, Teasdale G. Recovery of vision following treatment of pituitary tumours: application of a new system of assessment to patients treated by transsphenoidal operation. *Acta Neurochir (Wien)*. 1983;68:175–186.
35. Lennerstrand G. Visual recovery after treatment for pituitary adenoma. *Acta Ophthalmol (Copenh)*. 1983;61:1104–1117.
36. Gnanalingham KK, Bhattacharjee S, Pennington R, Ng J, Mendoza N. The time course of visual field recovery following transphenoidal surgery for pituitary adenomas: predictive factors for a good outcome. *J Neurol Neurosurg Psychiatry*. 2005;76:415–419.
37. Cohen AR, Cooper PR, Kupersmith MJ, Flamm ES, Ransohoff J. Visual recovery after transsphenoidal removal of pituitary adenomas. *Neurosurgery*. 1985;17:446–452.
38. Yoneoka Y, Hatase T, Watanabe N, et al. Early morphological recovery of the optic chiasm is associated with excellent visual outcome in patients with compressive chiasmal syndrome caused by pituitary tumors. *Neurol Res*. 2015;37:1–8.
39. Prieto R, Pascual JM, Barrios L. Optic chiasm distortions caused by craniopharyngiomas: clinical and magnetic resonance imaging correlation and influence on visual outcome. *World Neurosurg*. 2015;83:500–529.
40. Pardoe HR, Abbott DF, Jackson GD, et al. Alzheimer's disease neuroimaging, sample size estimates for well-powered cross-sectional cortical thickness studies. *Hum Brain Mapp*. 2013;34:3000–3009.
41. You Y, Gupta VK, Graham SL, Klistorner A. Anterograde degeneration along the visual pathway after optic nerve injury. *PLoS One*. 2012;7:e52061.

Investigative Ophthalmology & Visual Science